

## Molecular second- and third-order polarizabilities from measurements of second-harmonic generation in gases\*

J. F. Ward and Irving J. Bigio†

*The Harrison M. Randall Laboratory of Physics, The University of Michigan, Ann Arbor, Michigan 48104*

(Received 15 May 1974)

The temperature dependence of dc electric-field-induced optical second-harmonic generation has been measured for  $\text{CH}_4$ ,  $\text{CH}_3\text{F}$ ,  $\text{CH}_2\text{F}_2$ ,  $\text{CHF}_3$ ,  $\text{CF}_4$ ,  $\text{CClF}_3$ , and  $\text{CBrF}_3$ . For each molecule, experiments yield the second-order polarizability  $\bar{\chi}(-2\omega; \omega, \omega)$  and the third-order polarizability  $\bar{\chi}(-2\omega; 0, \omega, \omega)$ . Both independent nonzero spatial components of each are measured. The bond-additivity model is shown to work well ( $\pm 15\%$ ) for third-order polarizabilities but poorly (discrepancies of about a factor of two) for second-order polarizabilities.

### I. INTRODUCTION

We have derived values for second- and third-order electric polarizabilities (hyperpolarizabilities) for a selection of halogenated methanes from measurements of the temperature dependence of dc electric-field-induced second-harmonic generation. Previous studies<sup>1,2</sup> of dc electric-field-induced second-harmonic generation in gases have been made at a fixed temperature. Thus, in order to determine the separate contributions to the effect of the second- and third-order polarizabilities, it was necessary either to estimate the third-order contribution theoretically,<sup>1</sup> or to obtain additional data from another optical mixing experiment.<sup>2</sup> The scheme we have employed for obtaining the two hyperpolarizabilities is more direct because it does not make any assumptions regarding the frequency dependence of hyperpolarizabilities. In addition, our experimental method avoids uncertainties arising from recalibration of the apparatus for a second optical mixing process.

The molecules investigated here are among the simplest systems that exhibit a second-order polarizability. Whereas calculations thought to be good to 1% have been made for third-order polarizabilities of the helium atom,<sup>3</sup> the few second-order polarizabilities that have been calculated for molecules<sup>4</sup> typically disagree with experiment by a factor of 3 or more. Thus we believe that halogenated methane molecules have the ideal level of complexity for use in a study directed toward an improved understanding of nonlinear coefficients. In addition, the ability to study a series of related molecules allows a direct investigation of the bond-additivity model,<sup>5</sup> which is of importance in the understanding of the nonlinear coefficients of crystals.<sup>6</sup>

Molecules in a gas subjected to a dc electric field and an optical electric field at frequency  $\omega$  develop an induced dipole moment at the second-

harmonic frequency. The average induced dipole moment per molecule  $\bar{p}^{2\omega}$  may be written

$$\bar{p}_F^{2\omega} = \frac{3}{2} \chi_{FGHM}^e(-2\omega; 0, \omega, \omega) E_G^0 E_H^0 E_M^0, \quad (1)$$

where  $\chi_{FGHM}^e(-2\omega; 0, \omega, \omega)$  is an effective molecular hyperpolarizability, the  $E$ 's are electric field amplitudes at frequencies indicated by superscripts, and  $F, G, H, M$  stand for  $X, Y$ , or  $Z$  in the laboratory coordinate frame. The effective hyperpolarizability includes, in addition to the third-order dc electric-field-induced second-harmonic hyperpolarizability, a contribution from the second-order polarizability. This is nonzero in the case of molecules with permanent dipole moments ( $\mu$ ) which undergo temperature-dependent partial alignment by the dc field. The two contributions may be written explicitly:

$$\begin{aligned} \chi_{FGHM}^e(-2\omega; 0, \omega, \omega) = & \bar{\chi}_{FGHM}(-2\omega; 0, \omega, \omega) \\ & + (\mu/9kT) \bar{\chi}_{FGHM}(-2\omega; \omega, \omega). \end{aligned} \quad (2)$$

The laboratory-frame averaged hyperpolarizabilities of Eq. (2) are related to molecular second- and third-order polarizabilities  $\chi_{ijkl}(-2\omega; 0, \omega, \omega)$  and  $\chi_{ikl}(-2\omega; \omega, \omega)$ , respectively, by<sup>1,7</sup>

$$\begin{aligned} \bar{\chi}_{FGHM}(-2\omega; 0, \omega, \omega) = & \langle \Phi_{Fi} \Phi_{Gj} \Phi_{Hk} \Phi_{Ml} \rangle \\ & \times \chi_{ijkl}(-2\omega; 0, \omega, \omega) \end{aligned} \quad (3)$$

and

$$\begin{aligned} \chi_{FGHM}(-2\omega; \omega, \omega) = & \langle \Phi_{Fi} \Phi_{Gz} \Phi_{Hk} \Phi_{Ml} \rangle \\ & \times \chi_{ikl}(-2\omega; \omega, \omega), \end{aligned} \quad (4)$$

where  $i, j, k, l$  stand for  $x, y$ , and  $z$  in the molecular coordinate frame,  $\hat{z}$  has been placed along the dipole moment, and the expressions in angular brackets are isotropic averages of products of direction cosines which have been tabulated by Cyvin *et al.*<sup>8</sup> Details of conventions used here in defining molecular hyperpolarizabilities are dis-

cussed in Refs. 9 and 10.

In deriving Eqs. (2)–(4) it has been assumed that both the energy of the permanent dipole in the dc field,  $\mu E^0$ , and the rotational energy  $hcB$  are negligible compared with thermal energies  $kT$ . In fact, in these experiments  $hcB/kT$  is less than  $4 \times 10^{-3}$ ,  $\mu E^0/kT$  is about  $10^{-3}$ , and effects due to these deviations<sup>11</sup> from zero are negligible compared to experimental uncertainties. In addition, the difference between local and applied electric fields and the effects of intermolecular interactions under the conditions of these experiments have been shown<sup>12</sup> to be negligible.

The laboratory-frame coefficients of Eqs. (2)–(4) are subject to the symmetry restrictions appropriate to the macroscopic isotropy of the gas. This implies that there are only two independent nonzero spatial components for each hyperpolarizability. We chose the  $YYYY$  component which is measured with the optical and dc electric fields parallel ( $\parallel$ ) and the  $YYXX$  component which is measured with the optical and dc electric fields perpendicular ( $\perp$ ). It is therefore convenient to introduce the following abbreviated notation:

$$\chi_{\parallel}^e \equiv \chi_{YYYY}^e(-2\omega; 0, \omega, \omega), \quad (5)$$

$$\chi_{\perp}^e \equiv \chi_{YYXX}^e(-2\omega; 0, \omega, \omega), \quad (6)$$

$$R^e \equiv \chi_{\parallel}^e / \chi_{\perp}^e, \quad (7)$$

$$\chi_{\parallel}^{(3)} \equiv \bar{\chi}_{YYYY}^{(3)}(-2\omega; 0, \omega, \omega), \quad (8)$$

$$\chi_{\perp}^{(3)} \equiv \bar{\chi}_{YYXX}^{(3)}(-2\omega; 0, \omega, \omega), \quad (9)$$

$$R^{(3)} \equiv \chi_{\parallel}^{(3)} / \chi_{\perp}^{(3)}, \quad (10)$$

$$\chi_{\parallel}^{(2)} \equiv \bar{\chi}_{YYYY}^{(2)}(-2\omega; \omega, \omega), \quad (11)$$

$$\chi_{\perp}^{(2)} \equiv \bar{\chi}_{YYXX}^{(2)}(-2\omega; \omega, \omega), \quad (12)$$

$$R^{(2)} \equiv \chi_{\parallel}^{(2)} / \chi_{\perp}^{(2)}. \quad (13)$$

From the current experiments we extract information on the two spatial components of both the second- and third-order polarizabilities and present the data in terms of  $\chi_{\parallel}^{(3)}$ ,  $R^{(3)}$ ,  $\chi_{\parallel}^{(2)}$ , and  $R^{(2)}$ . The apparatus and experiments are presented in Sec. II and the results are discussed in Sec. III.

## II. EXPERIMENTAL

The experimental apparatus is similar to that described previously<sup>13</sup> and a schematic diagram is shown in Fig. 1. A 1-MW ruby laser beam is brought to a focus in the gas under observation, between cylindrical electrodes maintained at a potential difference  $V_0$ . The magnitude of the applied transverse dc electric field at the focus was in the range 12–65 esu. The angle of the optical electric field with respect to the dc electric field is controlled by a rotatable half-wave plate traversed by

the beam before it enters the gas cell. dc electric-field-induced second-harmonic radiation generated in the gas is detected by a photomultiplier, integrated during the laser pulse, and recorded ( $V_s$ ). The laser-beam intensity is monitored via the second-harmonic generation in a quartz crystal which is similarly detected and recorded ( $V_m$ ). Typically,  $10^3$ – $10^4$  second-harmonic photons are generated in the gas during each laser shot, corresponding to 5–500 photoelectrons ejected from the photomultiplier cathode. The temperature of the gas cell can be controlled within the range 295–600 °K.

It is convenient to define a quantity  $S$  (which will be referred to as the “signal”) in terms of measured quantities

$$S \equiv V_s / V_m V_0^2. \quad (14)$$

It can be shown (see Ref. 14) that with the gas density adjusted to yield maximum harmonic the hyperpolarizability is related to the signal by

$$S = \text{const} \times |\chi^e / \Delta k_0|^2, \quad (15)$$

where  $\chi^e$  is  $\chi_{\parallel}^e$  or  $\chi_{\perp}^e$  depending on the wave-plate setting and the constant is independent of the gas used.  $\Delta k_0$  is a measure of the optical dispersion of the gas and is related to the wave vectors for the fundamental,  $k_0^\omega$ , and harmonic,  $k_0^{2\omega}$ , by

$$\Delta k_0 = 2k_0^\omega - k_0^{2\omega}. \quad (16)$$

The subscripts zero here indicate quantities evaluated for a gas at a molecular number density of Loschmidt's number per  $\text{cm}^3$ .

The experiment involves three types of measurement which will now be described in turn.

### A. $\chi_{\parallel}^e$ at ambient temperature

Signals were measured for helium and for a halogenated methane gas alternately, with the op-

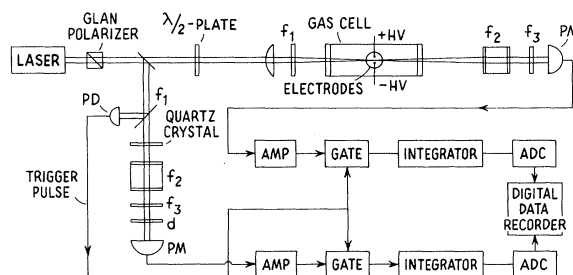


FIG. 1. Schematic diagram of the apparatus: d, diffuser;  $f_1$ , red filter;  $f_2$ , aqueous  $\text{CuSO}_4$  filter;  $f_3$ ,  $2\omega$ -interference filter; PM, photomultiplier RCA type 4818; PD, photodiode RCA type 922. There is provision for controlling and measuring the gas cell temperature in the range 295–600 °K.

tical electric field parallel to the dc electric field and with the gas at ambient temperature ( $T_a = 295^\circ\text{K}$ ). Gas pressures for optimum harmonic generation<sup>15</sup> vary inversely with  $\Delta k_0$  and, except for helium (40 atm), are in the range of 0.4 atm for  $\text{CBrF}_3$  to 1.7 atm for  $\text{CF}_4$ . Sitz and Yaris<sup>3</sup> have calculated the third-order coefficient for helium (there is no second-order contribution) and the resulting value, thought to be good to 1%, is

$$\chi_{YXYX}(-2\omega; 0, \omega, \omega) (\text{helium}) = 3.79 \times 10^{-39} \text{ esu/atom.} \quad (17)$$

The measured signals together with values of  $\Delta k_0$  from the literature<sup>15</sup> and Eqs. (15) and (17) yield the  $\chi_{\parallel}^e$  for halogenated methanes shown in Table I. Standard deviations are in the range 3–8% and arise largely from uncertainties in  $\Delta k_0$ , photon-counting statistics, and drifts in apparatus parameters. No allowance for the uncertainty in the calculated helium coefficient has been included. The signs of the coefficients given in Table I are taken from Ref. 1 and were obtained by studying harmonic generation in binary mixtures of gases and assuming that for argon the sign of the dc-induced optical second-harmonic coefficient is the same as the measured sign of the Kerr coefficient.<sup>16</sup>

#### B. $R^e$ at ambient temperature

The variation of signal with optical-electric-field orientation was measured for each gas at ambient temperature to determine the ratio  $R^e$  of coefficients which has been defined in Eq. (7). The

method is described in greater detail in Ref. 13, which presents similar measurements in the inert gases together with a careful analysis of systematic effects.

Results are shown in Table I with uncertainties typically  $\pm 1\frac{1}{2}\%$  which are largely due to photon-counting statistics and nonlinearities in the electronics.

#### C. $\chi_{\parallel}^e$ and $\chi_{\perp}^e$ as a function of temperature

The gas cell was heated to several temperatures in the range 295–600°K and, at each temperature signals were measured with the optical field first parallel to and then perpendicular to the dc field.

For a given gas, the square root of the signal  $\sqrt{S}$  is proportional to the modulus of  $\chi^e$  [see Eq. (15)] but the sign of  $\chi^e$  is ambiguous. Figure 2 shows a plot of  $\sqrt{S}$  versus the inverse temperature  $1/T$  for  $\text{CBrF}_3$ . The three points at low temperature have been arbitrarily plotted with  $\sqrt{S}$  positive and the other two points have then been plotted with  $\sqrt{S}$  negative for qualitative consistency with the linear dependence of  $\chi^e$  on  $1/T$  predicted by Eq. (2). The crossover temperature  $T_{\parallel}$ , where  $\chi_{\parallel}^e$  becomes zero, constitutes the result of the experiment and is independent of the choice of signs. Qualitatively we see that  $1/T_{\parallel}$  for  $\text{CBrF}_3$  lies between 0 and  $1/T_a$  (as is the case for all the dipolar gases we studied here), which implies that  $\chi_{\parallel}^{(3)}$  and  $\chi_{\parallel}^{(2)}$  are of opposite sign, with the  $\chi_{\parallel}^{(2)}$  contribution dominating at ambient temperature. [The sign of  $\chi_{\parallel}^{(2)}$  is to be interpreted in conjunction with the coordinate con-

TABLE I. Experimental data (discussed in the text) and  $\Delta k_0$  from the literature.

	$-\Delta k_0$ ( $\text{cm}^{-1}$ )	$\chi_{\parallel}^e(T_a)$ ( $10^{-39}$ esu/mol)	$R^e(T_a)$	$1/T_{\parallel}$ ( $10^{-3}$ °K $^{-1}$ )	$1/T_{\perp}$ ( $10^{-3}$ °K $^{-1}$ )
$\text{CH}_4$	$4.1 \pm 0.3^a$	$+258 \pm 19$	$3.05 \pm 0.05$	...	...
$\text{CH}_3\text{F}$	$3.34 \pm 0.10^b$	$-992 \pm 71$	$3.045 \pm 0.05$	$0.66 \pm 0.06$	$0.66 \pm 0.07$
$\text{CH}_2\text{F}_2$	$2.84 \pm 0.12^c$	$-815 \pm 36$	$3.03 \pm 0.05$	$0.54 \pm 0.03$	$0.51 \pm 0.05$
$\text{CHF}_3$	$2.42 \pm 0.07^d$	$-352 \pm 11$	$2.92 \pm 0.04$	$0.95 \pm 0.02$	$0.93 \pm 0.025$
$\text{CH}_4$	$2.03 \pm 0.05^e$	$+91 \pm 3$	$3.04 \pm 0.04$	...	...
$\text{CClF}_3$	$5.55 \pm 0.2^f$	$-99 \pm 4$	$2.89 \pm 0.06$	$2.57 \pm 0.015$	$2.58 \pm 0.03$
$\text{CBrF}_3$	$8.96 \pm 0.6^g$	$-437 \pm 29$	$2.94 \pm 0.04$	$2.00 \pm 0.02$	$2.00 \pm 0.035$
He	$0.0946^h$	...			

<sup>a</sup> Derived from data given in H. E. Watson and K. L. Ramaswamy, Proc. R. Soc. Lond. A **156**, 144 (1936).

<sup>b–g</sup> Measurements of  $\Delta k$  from Ref. 15 corrected to a molecular number density of Loschmidt's number per  $\text{cm}^3$  using virial data given in the following references.

<sup>b</sup> A. Michels, A. Visser, R. J. Lunbeck, and G. J. Wolkers, Physica **18**, 114 (1952).

<sup>c</sup> P. G. T. Fogg, P. A. Hanks, and J. D. Lambert, Proc. R. Soc. Lond. A **219**, 490 (1953).

<sup>d</sup> J. H. Dymond and E. B. Smith, Trans. Faraday Soc. **60**, 1378 (1964).

<sup>e</sup> D. R. Doushin, R. H. Harrison, R. T. Moore, and J. P. McCullough, J. Chem. Phys. **35**, 1357 (1961).

<sup>f</sup> Thermodynamic Properties of Freon-13 (E. I. DuPont de Nemours, Wilmington, Del., 1959).

<sup>g</sup> Includes an estimated correction of  $-5 \pm 5\%$  for the nonideal nature of the gas.

<sup>h</sup> C. R. Mansfield and E. R. Peck, J. Opt. Soc. Am. **59**, 199 (1969).

vention defined following Eq. (4).] Quantitatively, the ratio of third- and second-order hyperpolarizabilities can be written in terms of  $T_{\parallel}$  using Eq. (2):

$$1/T_{\parallel} = -9k\chi_{\parallel}^{(3)}/\mu\chi_{\parallel}^{(2)} \quad (18)$$

and similarly

$$1/T_{\perp} = -9k\chi_{\perp}^{(3)}/\mu\chi_{\perp}^{(2)}. \quad (19)$$

Measured values of  $1/T_{\parallel}$  and  $1/T_{\perp}$  are shown in Table I.

Results in a form convenient for discussion can be derived from the experimental data— $\chi_{\parallel}^e(T_a)$ ,  $R^e(T_a)$ ,  $T_{\parallel}$ ,  $T_{\perp}$ —using the following relations which follow from Eqs. (2), (5)–(13), (18), and (19):

$$\chi_{\parallel}^{(3)} = \frac{(1/T_{\parallel})\chi_{\parallel}^e(T_a)}{1/T_{\parallel} - 1/T_a}, \quad (20)$$

$$R^{(3)} = \chi_{\parallel}^{(3)}/\chi_{\perp}^{(3)} = \frac{(1/T_{\parallel})(1/T_{\perp} - 1/T_a)}{(1/T_{\perp})(1/T_{\parallel} - 1/T_a)} R^e(T_a), \quad (21)$$

$$\chi_{\parallel}^{(2)} = \frac{9k}{\mu} \frac{\chi_{\parallel}^e(T_a)}{(1/T_a - 1/T_{\parallel})}, \quad (22)$$

$$R^{(2)} = \chi_{\parallel}^{(2)}/\chi_{\perp}^{(2)} = \frac{(1/T_{\perp} - 1/T_a)}{(1/T_{\parallel} - 1/T_a)} R^e(T_a). \quad (23)$$

These results are given in Tables II and III, and discussed in Sec. III.

### III. DISCUSSION

#### A. Ratios of independent spatial components, $R^{(2)}$ and $R^{(3)}$

For all gases studied here,  $R^{(2)}$  and  $R^{(3)}$  (Tables II and III) each differ from 3 by amounts which are insignificant compared to the experimental uncertainties (1–10%). Moreover the experimental equality of  $1/T_{\parallel}$  and  $1/T_{\perp}$  together with Eqs. (21) and (23) implies more directly and with smaller uncertainty that, for each gas,  $R^{(3)}$  and  $R^{(2)}$  are equal.

It has been shown<sup>13</sup> that  $R$  is given by a relation of the form

$$R^{(2,3)} = 3(1 + C^{(2,3)}\omega^2/\omega_0^2 \dots), \quad (24)$$

where  $\omega_0$  is a characteristic frequency for the molecule and  $C$  is a numerical coefficient. Thus  $R$  becomes 3, as demanded by symmetry, in the limit  $\omega \rightarrow 0$ . The closeness of  $R^{(3)}$  to 3 for the inert gases,<sup>13</sup> although not understood, prepares us for the same result here. Although there is no theoretical estimate for  $C^{(2)}$  we find it surprising that  $R^{(2)}$  is indistinguishable from 3 and from  $R^{(3)}$ .

#### B. Third-order polarizabilities, $\chi_{\parallel}^{(3)}$

Experimental results for  $\chi_{\parallel}^{(3)}$  are given in Table II. Other experimental third-order polarizabilities

taken from the literature are also given for comparison: Kerr-effect measurements by Buckingham and Orr<sup>16</sup> and measurements by Hauchecorne, Keherve, and Mayer<sup>2</sup> of dc electric-field-induced optical harmonic generation and optical mixing coefficients. The hyperpolarizabilities for a particular molecule might be expected to vary by as much as (10–20)% from process to process since different sets of frequencies are involved. We believe that this variation together with experimental uncertainties (which we estimate where necessary) are sufficient to explain the range of data observed.

It is interesting to compare our results with predictions based on the bond-additivity model. This model has been used (with varying degrees of success) to understand the variation from molecule to molecule of permanent dipole moments, polarizabilities, and hyperpolarizabilities.<sup>5</sup> It is also an essential feature of methods which have been used successfully to calculate second-harmonic coefficients for a wide range of crystals.<sup>6</sup> In the bond-additivity model a coefficient is ascribed to each individual bond, and it is assumed that the bond coefficient is independent of the other bonds in the molecule. The molecular coefficient is then synthesized by appropriate geometric combination of the bond contributions. In the specific case of third-order polarizabilities  $\chi^{(3)}$  (using fluorinated methanes as an example) this synthesis takes the form

$$\chi^{(3)}(\text{CH}_n\text{F}_{4-n}) = n\chi^{(3)}(\text{C-H bond}) + (4-n)\chi^{(3)}(\text{C-F bond}), \quad (25)$$

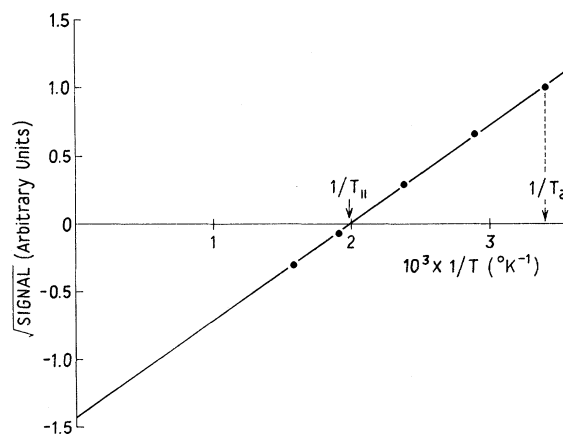


FIG. 2. Typical data for the temperature dependence of  $\chi^e$ . The square root of the signal (the question of sign is discussed in the text) is shown plotted vs the inverse temperature. This case is for  $\text{CBrF}_3$  with the optical and dc fields parallel.  $T_{\parallel}$  is the temperature at which the second- and third-order contributions cancel, yielding zero for the effective coefficient.  $T_a$  is ambient temperature, and uncertainties are comparable with the dot size.

TABLE II. Third-order polarizabilities in units of  $10^{-39}$  esu/molecule and the ratio of spatial components  $R^{(3)}$  defined in Eq. (10). Bond-additivity estimates are based on values given in parentheses.

	$R^{(3)}$	Expt	$\chi_{  }^{(3)}$ Bond add.	Other experimental $\chi$ 's		
CH <sub>4</sub>	3.05 ± 0.05	258 ± 19	(258)	244 ± 12 <sup>a</sup>	260 <sup>b</sup>	285 <sup>c</sup>
CH <sub>3</sub> F	3.04 ± 0.44	239 ± 30	216			
CH <sub>2</sub> F <sub>2</sub>	3.24 ± 0.37	154 ± 11	174			
CHF <sub>3</sub>	3.01 ± 0.12	136 ± 6	133			
CF <sub>4</sub>	3.04 ± 0.04	91 ± 3	(91)	125 ± 7 <sup>a</sup>		153 <sup>c</sup>
CClF <sub>3</sub>	2.84 ± 0.13	306 ± 13				
CBrF <sub>3</sub>	2.94 ± 0.11	625 ± 43				

<sup>a</sup> Kerr coefficient from Ref. 16.

<sup>b</sup>  $\bar{\chi}_{Y Y Y Y}(-2\omega; 0, \omega, \omega)$  from Ref. 2.

<sup>c</sup>  $\bar{\chi}_{Y Y Y Y}(-2\omega + \omega_s; -\omega_s, \omega, \omega)$  from Ref. 2.

so that

$$\chi^{(3)}(\text{CH}_4) = 4\chi^{(3)}(\text{C-H bond}) \quad (26)$$

and

$$\chi^{(3)}(\text{CF}_4) = 4\chi^{(3)}(\text{C-F bond}). \quad (27)$$

These equations have been used to estimate  $\chi_{||}^{(3)}$  for CH<sub>3</sub>F, CH<sub>2</sub>F<sub>2</sub>, and CHF<sub>3</sub> from measured values for CH<sub>4</sub> and CF<sub>4</sub>, and the results are shown in Table II. The bond-additivity estimates are within 15% (or about one standard deviation) of the measured values, which suggests that the bond-additivity approximation is currently a useful basis for the calculation of third-order polarizabilities.

It is interesting to note that the bond-additivity equation for the linear polarizability, and therefore for  $\Delta k_0$ , is analogous to Eq. (25); applying this to the data given for  $\Delta k_0$  in Table I shows that the fit is good.

We are not aware of any *ab initio* calculations for these third-order polarizabilities.

### C. Second-order polarizabilities, $\chi_{||}^{(2)}$

Second-order polarizabilities are presented in Table III along with other experimental and theoretical data for comparison. Hauchecorne *et al.*<sup>2</sup> have measured  $\chi^{(2)}$  for CHF<sub>3</sub> (and for other molecules not of direct interest here) by subtracting from  $\chi^e$  the coefficient for another process with no second-order contribution. Their value is substantially smaller than ours but of the same sign. Estimating the uncertainties in their measurement we believe our results are not inconsistent with theirs. The Kerr coefficient for CHF<sub>3</sub> measured by Buckingham and Orr,<sup>4</sup> however, is three times larger than the dc-induced second-harmonic coefficient and of *opposite* sign, as first pointed out by Hauchecorne *et al.*<sup>2</sup> Since different frequencies are involved in the third-order processes being compared [ $\chi^e(-2\omega; 0, \omega, \omega)$  and  $\chi^e(-\omega; 0, 0, \omega)$ ] we would not be surprised if the coefficients differed by as much as 20%. A *large* difference, like that observed here, could be caused by a resonant ef-

TABLE III. Second-order polarizabilities in units of  $10^{-33}$  esu/molecule and the ratio of spatial components  $R^{(2)}$  defined in Eq. (13). Bond-additivity estimates are based on the value given in parentheses. Values of the molecular permanent electric-dipole moments  $\mu$  from the literature are also shown.

	$\mu^a$ ( $10^{-18}$ esu cm)	$R^{(2)}$	Expt	$\chi_{  }^{(2)}$ Bond add.	Other $\chi$ data		
CH <sub>4</sub>	0	...	...				
CH <sub>3</sub> F	1.85	3.04 ± 0.11	-244 ± 18	(-244)	-250 ± 132 <sup>b</sup>	-25.9 <sup>d</sup>	-80 <sup>e</sup>
CH <sub>2</sub> F <sub>2</sub>	1.97	3.06 ± 0.08	-180 ± 8	-282	-55 ± 13 <sup>b</sup>	-34.2 <sup>d</sup>	
CHF <sub>3</sub>	1.65	2.94 ± 0.06	-108 ± 4	-244	+364 ± 135 <sup>b</sup>	-74 <sup>c</sup>	+30.2 <sup>d</sup>
CF <sub>4</sub>	0	...	...				
CClF <sub>3</sub>	0.50	2.86 ± 0.13	-296 ± 12				
CBrF <sub>3</sub>	0.65	2.94 ± 0.09	-598 ± 40				

<sup>a</sup> R. D. Nelson, Jr., D. R. Lide, Jr., and A. A. Maryott, Natl. Stand. Ref. Data Ser. 10 (1967).

<sup>b</sup> Kerr coefficients from Ref. 16.

<sup>c</sup>  $(9kT/\mu)[\bar{\chi}_{Y Y Y Y}^e(-2\omega; 0, \omega, \omega) - \bar{\chi}_{Y Y Y Y}^e(-2\omega + \omega_s; -\omega_s, \omega, \omega)]$  from Ref. 2.

<sup>d</sup> N. S. Hush and M. L. Williams, Theor. Chim. Acta 25, 346 (1972), calculated value of  $\chi(0; 0, 0)$ .

<sup>e</sup> G. P. Arrighini, M. Maestro, and R. Moccia, Symp. Faraday Soc. 2, 48 (1968), calculated values of  $\chi(0; 0, 0)$ .

fect, but we are not aware of the existence of such a resonance. There is also a discrepancy between our data and the Kerr data for  $\text{CH}_2\text{F}_2$ , but for  $\text{CH}_3\text{F}$  the results are consistent.

Molecular orbital calculations of dc hyperpolarizabilities, reported in the literature, give results (see Table III) which are substantially smaller than our measured values.

In the bond-additivity model  $\chi^{(2)}$  for a molecule is related to the bond contributions via geometric factors. For fluorinated methanes (ignoring small deviations from tetrahedral bond angles) the relation is

$$\chi^{(2)}(\text{CH}_n\text{F}_{4-n}) = K \times [\chi^{(2)}(\text{C-H bond}) - \chi^{(2)}(\text{C-F bond})],$$

$$K = 0, \quad n = 0, 4,$$

$$K = 1, \quad n = 1, 3,$$

$$K = 2/\sqrt{3}, \quad n = 2. \quad (28)$$

Equation (28) can be used to estimate  $\chi_{\parallel}^{(2)}$  for  $\text{CH}_2\text{F}_2$  and  $\text{CHF}_3$  from the measured value for  $\text{CH}_3\text{F}$ . These bond-additivity estimates are shown in Table III and differ by about a factor of 2 (1.5 for  $\text{CH}_2\text{F}_2$  and 2.3 for  $\text{CHF}_3$ ) from the measured  $\chi_{\parallel}^{(2)}$  values, whereas experimental uncertainties are less than 10%. The Kerr-effect results, however, are even less satisfactorily reproduced by the bond-additivity model. Of course, it is intrinsically difficult to derive an accurate result for a quantity which depends on the *difference* between two comparable numbers as indicated for  $\chi^{(2)}$  by Eq. (28), while in the case of  $\chi^{(3)}$  a *sum* is involved, as indicated in Eq. (25). Corrections to Eq. (28) due to deviation from tetrahedral bond angles become significant if the cancellation between C-H and C-F bond contribution is severe. However, it

does not seem likely that this could explain factors-of-2 discrepancies between bond-additivity data and experimental values.

#### IV. CONCLUSIONS

We have established an effective technique based on the temperature dependence of electric-field-induced optical second-harmonic generation for making accurate measurements of second- and third-order polarizabilities for molecules. Both independent nonzero spatial components of each hyperpolarizability are measured.

Our data are consistent with the limited amount of other experimental data with the conspicuous exception that  $\chi^{(2)}$  for  $\text{CH}_2\text{F}_2$  and  $\text{CHF}_3$  differs greatly from the Kerr-effect measurements.

Molecular orbital calculations, where available, agree poorly with experiment.

The surprising closeness to 3 of the ratio of the two independent spatial components of both second- and third-order polarizabilities for all molecules studied remains to be explained.

Bond-additivity works well for the third-order polarizabilities (to within ~15%) but much less well for second-order polarizabilities (about a factor of 2). Calculations of second-order susceptibilities for crystals, in which the bond-additivity model plays an essential role, agree with measurements to substantially higher accuracy than the factor of 2 discussed above. The reasons for this remain to be explained. The bond-additivity model offers such a simplification in calculations of hyperpolarizabilities that it would be desirable to improve the model by including small contributions arising from bond-bond interactions. We plan to extend these measurements to a wider range of molecules.

\*Research supported in part by the Air Force Office of Scientific Research under Grant No. 72-2302.

†Present address: Los Alamos Scientific Laboratory, Group L-7, P. O. Box 1663, Los Alamos, N.M. 87544.

<sup>1</sup>R. S. Finn and J. F. Ward, *J. Chem. Phys.* **60**, 454 (1974).

<sup>2</sup>G. Hauchecorne, F. Kerherve, and G. Mayer, *J. Phys. (Paris)* **32**, 47 (1971). In quoting data from this reference we have used the alternative calibration discussed by the authors. This involves normalizing with respect to the measured Kerr coefficient for argon (see Ref. 16) and seems to be more consistent with other normalizations involved in data discussed here.

<sup>3</sup>P. Sitz and R. Yaris, *J. Chem. Phys.* **49**, 3546 (1968).

<sup>4</sup>G. P. Arrighini, M. Maestro, and R. Moccia, *Symp. Faraday Soc.* **2**, 48 (1968); N. S. Hush and M. L. Williams, *Theor. Chim. Acta.* **25**, 346 (1972).

<sup>5</sup>For a discussion see A. D. Buckingham and B. J. Orr, *Q. Rev. Chem. Soc.* **21**, 195 (1967).

<sup>6</sup>See, for example, B. F. Levine, *Phys. Rev. B* **7**, 2600 (1973); C. L. Tang and C. Flytzanis, *Phys. Rev. B* **4**, 2520 (1971); D. S. Chemla, R. F. Begley, and R. L. Byer, *IEEE J. Quantum Electron* **10**, 71 (1974).

<sup>7</sup>Irving J. Bigio, Ph.D. thesis (University of Michigan, 1974) (unpublished).

<sup>8</sup>S. J. Cyvin, J. E. Rauch, and J. C. Decius, *J. Chem. Phys.* **43**, 4083 (1965).

<sup>9</sup>J. F. Ward and G. H. C. New, *Phys. Rev.* **185**, 57 (1969).

<sup>10</sup>B. J. Orr and J. F. Ward, *Mol. Phys.* **20**, 513 (1971).

<sup>11</sup>A. D. Buckingham and B. J. Orr, *Proc. R. Soc. Lond. A* **305**, 259 (1968); S. Kielich, *IEEE J. Quantum Electron* **5**, 562 (1969).

<sup>12</sup>R. S. Finn, Ph.D. thesis (University of Michigan, 1971) (unpublished).

- <sup>13</sup>Irving J. Bigio and J. F. Ward, Phys. Rev. A 9, 35 (1974).
- <sup>14</sup>R. S. Finn and J. F. Ward, Phys. Rev. Lett. 26, 285 (1971).
- <sup>15</sup>R. S. Finn and J. F. Ward, Appl. Opt. 11, 2103 (1972). In this reference, departures from ideal-gas behavior are ignored. Data for  $\Delta k_0$  shown in Table I are consistent with the definition given here, before Eq. (16), and include a correction (-2 to -7%) for the nonideal behavior of the gases, evaluated using virial data referenced in the caption to Table I.
- <sup>16</sup>A. D. Buckingham and B. J. Orr, Trans. Faraday Soc. 65, 673 (1969).